

Measurement of Angular Distribution for the ${}^8\text{Li}(p,d){}^7\text{Li}$ Reaction *

LI Yun-Ju(李云居)^{1,2**}, LI Zhi-Hong(李志宏)¹, GUO Bing(郭冰)¹, WANG You-Bao(王友宝)¹,
BAI Xi-Xiang(白希祥)¹, SU Jun(苏俊)¹, LIAN Gang(连钢)¹, ZENG Sheng(曾晟)¹,
WANG Bao-Xiang(王宝祥)¹, QIN Xing(秦星)^{1,3}, JIANG Chao(蒋超)^{1,3},
LIU Wei-Ping(柳卫平)¹, ZHAO Wei-Juan(赵维娟)²

¹China Institute of Atomic Energy, Beijing 102413

²Institute of Physical Engineering, Zhengzhou University, Zhengzhou 450052

³Institute of Modern Physics, Shanxi Normal University, Linfen 041004

(Received 26 November 2007)

The ${}^8\text{Li}(p,d){}^7\text{Li}$ reaction plays an important role in the inhomogeneous Big Bang nucleosynthesis and in the seed-nuclide production phase for the r-process. For the first time, its angular distribution at backward angles was measured in inverse kinematics at $E_{\text{c.m.}} = 4.0$ MeV by using an ${}^8\text{Li}$ secondary beam. The result of measurement includes the contributions of ${}^8\text{Li}(p,d_0){}^7\text{Li}$ and ${}^8\text{Li}(p,d_1){}^7\text{Li}^*$. The ${}^8\text{Li}(p,d_0){}^7\text{Li}$ component is estimated to be 40%~58% in the mixture angular distribution by analysing the measured result.

PACS: 25.60.Je, 26.35.+c, 23.20.En, 25.60.-t

In recent years, significant efforts have been paid to inhomogeneous Big Bang nucleosynthesis (IBBNs)^[1,2] and the r-process which synthesizes roughly half of all elements heavier than iron.^[3,4] ${}^8\text{Li}(p,d){}^7\text{Li}$ is one of the key reactions involved in the reaction networks for the IBBNs and for the seed-nuclide production of the r-process. In the IBBNs the stability gap at mass number $A = 8$ can be bypassed with the reaction chains containing unstable nucleus ${}^8\text{Li}$ to synthesize $A > 8$ nuclides.^[5] Thus the IBBNs predict relatively higher abundances for heavier nuclides in primordial nucleosynthesis than the standard model does.^[6,7] The production of $A > 8$ nuclides depends on the abundance of ${}^8\text{Li}$ during primordial nucleosynthesis.

In the reaction networks of nucleosynthesis, ${}^8\text{Li}$ is produced by ${}^7\text{Li}(n,\gamma)$ and ${}^7\text{Li}(d,p)$, and destroyed by its β -decay as well as by the reactions such as ${}^8\text{Li}(\alpha,n){}^{11}\text{B}$, ${}^8\text{Li}(d,n){}^9\text{Be}$, ${}^8\text{Li}(d,p){}^9\text{Li}$, ${}^8\text{Li}(d,t){}^7\text{Li}$, ${}^8\text{Li}(d,\alpha){}^6\text{He}$, ${}^8\text{Li}(p,d){}^7\text{Li}$, ${}^8\text{Li}(p,t){}^6\text{Li}$, ${}^8\text{Li}(p,\alpha){}^5\text{He}$, ${}^8\text{Li}(p,n\alpha){}^4\text{He}$, ${}^8\text{Li}(p,\gamma){}^9\text{Be}$ and ${}^8\text{Li}(n,\gamma){}^9\text{Li}$. Most of these reactions have been measured in the past years.^[8-11] At CIAE, the angular distributions of the ${}^8\text{Li}(d,p){}^9\text{Li}$ and ${}^8\text{Li}(d,n){}^9\text{Be}$ reactions were measured, and the astrophysical ${}^8\text{Li}(n,\gamma){}^9\text{Li}$ reaction rate and the astrophysical ${}^8\text{Li}(p,\gamma){}^9\text{Be}$ S-factor were deduced.^[12-14] The former result shows that the ${}^8\text{Li}(n,\gamma){}^9\text{Li}$ direct capture reaction may play an important role in the astrophysical environments of inhomogeneous Big Bang and type II supernovae. The ${}^8\text{Li}(p,d){}^7\text{Li}$ reaction is predicted to have large cross section and may be one of the main reactions to destroy ${}^8\text{Li}$. At low energies of astrophysical relevance, both the ground and first excited states in ${}^7\text{Li}$ can be

populated through this reaction due to the low excitation energy (0.477 MeV) of the first excited state in ${}^7\text{Li}$, and thus can contribute to destroying ${}^8\text{Li}$.

In this Letter, we report the first measurement of the ${}^8\text{Li}(p,d){}^7\text{Li}$ reaction leading to the ground and first excited states in ${}^7\text{Li}$ by using a ${}^8\text{Li}$ secondary beam. The experimental result is also compared with that deduced from the ${}^7\text{Li}(d,p_0){}^8\text{Li}$ reaction according to the principle of detailed balance.

The experiment was carried out at the radioactive nuclear beam facility of the HI-13 tandem accelerator, Beijing.^[15,16] A 44-MeV ${}^7\text{Li}$ primary beam from the tandem accelerator impinged on a 4.8-cm-long deuterium gas cell at the pressure of 1.55 atm, and the ${}^8\text{Li}$ secondary beam was produced via ${}^2\text{H}({}^7\text{Li}, {}^8\text{Li}){}^1\text{H}$ reaction. The front and rear windows of the gas cell were Havar foils with the thickness of 1.9 mg/cm². After the magnetic separation with a dipole and the focalization with a quadruple doublet respectively, the beam was collimated by a $\phi 7 - \phi 3$ mm collimator complex. A set of $\Delta E - E$ telescope of silicon detectors was arranged on a movable ladder behind the collimator for beam-tuning. The energy of the ${}^8\text{Li}$ secondary beam was 39.8 MeV, with the intensity of 3000 pps and purity of 78%~86%. The energy spread was measured to be 0.54 MeV (FWHM), and the beam angular divergence was about 0.3°. The main contaminant was ${}^7\text{Li}$ ions from Rutherford scattering of the primary beam in the gas cell windows and beam tube.

The layout of the experimental setup is shown in Fig.1. The beam were recorded with a silicon ΔE detector of 21.7 μm upstream of the secondary target to serve as beam normalization. A 1.93-mg/cm²-thick

*Supported by the National Basic Research Programme of China under Grant No 2007CB815003, the National Natural Science Foundation of China under Grant Nos 10675173 and 10705053.

** Email: li_yunju@ciae.ac.cn

© 2008 Chinese Physical Society and IOP Publishing Ltd

(CH₂)_n foil and a 1.9-mg/cm²-thick carbon foil were used to measure the ⁸Li(*p, d*)⁷Li reaction in inverse kinematics and to evaluate the background, respectively.

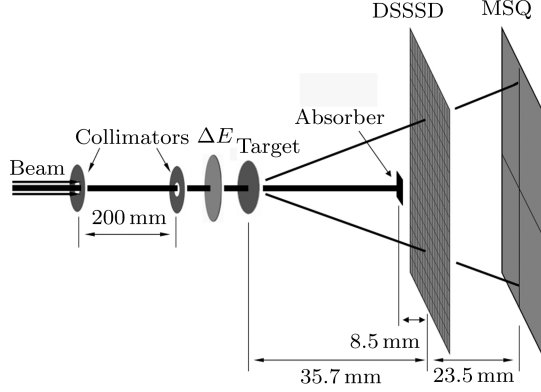


Fig. 1. Schematic layout of the experiment.

The maximum emission angles of deuteron and ⁷Li from the ⁸Li(*p, d*)⁷Li reaction were 42.6° and 11.2°, respectively. In order to remove the influence of their pile-up on the identification of reaction products, we used a set of $\Delta E - E$ telescope consisting of a 63- μ m-thick double sided silicon strip detector (DSSSD)^[17] and a 982- μ m-thick quadrant silicon detector (MSQ). Both the detectors have 50 mm \times 50 mm active area. The DSSSD is divided into 16 strips with 3 mm width on the front face by 0.1 mm gaps and 16 similar orthogonal strips on the back face, making up 256 pixels of 3 mm \times 3 mm each, to provide quasi-pixel two dimensional position information. Taking account of detecting the emitted deuterons and reducing the dead-time of data acquisition system, only a 10 \times 10 pixel array in the central part of DSSSD was used in the experiment. The MSQ is a 2 \times 2 array of individual active area, separated by a 0.1 mm cross gap. A 1 mm thick aluminium absorber with an area of 5.7 mm \times 5.7 mm was placed at 8.5 mm upstream from DSSSD to decrease radiation damage to DSSSD as well as the pile-up events induced by the incident beam. Restricted by the absorber and the 10 \times 10 pixel array, the angular acceptance for emitted deuterons was 8.4° \sim 30.8° in the laboratory frame.

The influence of ⁷Li ions in the beam on the measurement of the ⁸Li(*p, d*)⁷Li reaction can be negligible because the threshold energy of the ¹H(⁷Li, *d*)⁶Li reaction (about 40 MeV) is greater than the maximum energy of ⁷Li ions impinging on the (CH₂)_n target.

The accumulated numbers of incident ⁸Li ions are approximately 3.55×10^8 , and 1.23×10^8 for the (CH₂)_n and carbon targets, respectively. In order to select the deuteron events, a particle-identification (PID) function is defined. The ΔE distributions for both deuterons and protons in the two-dimensional

plot of $\Delta E - E$ are fitted as functions of E by using a third-order polynomial. The PID function is defined as

$$\text{PID} = \frac{\Delta E - f_p(E)}{f_d(E) - f_p(E)} + 1, \quad (1)$$

where $f_p(E)$ and $f_d(E)$ denote the fitted function as described above for protons and deuterons, respectively. As can clearly be seen from Fig. 2, the proton, deuteron and triton events are well identified with the PID function. The deuteron events from the carbon target are much less than those from the (CH₂)_n target, and thus can be subtracted as the background in the data analysis.

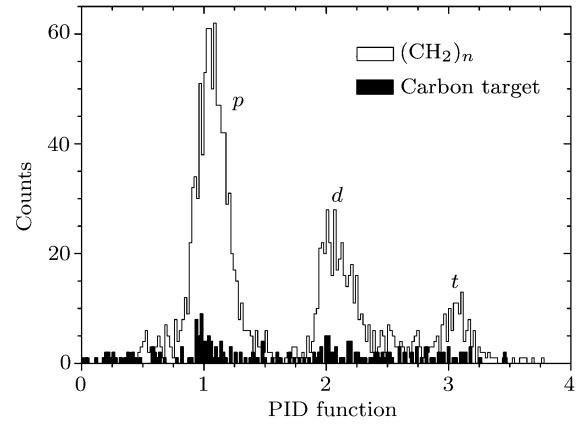


Fig. 2. Typical PID function from one strip of DSSSD for (CH₂)_n and carbon targets.

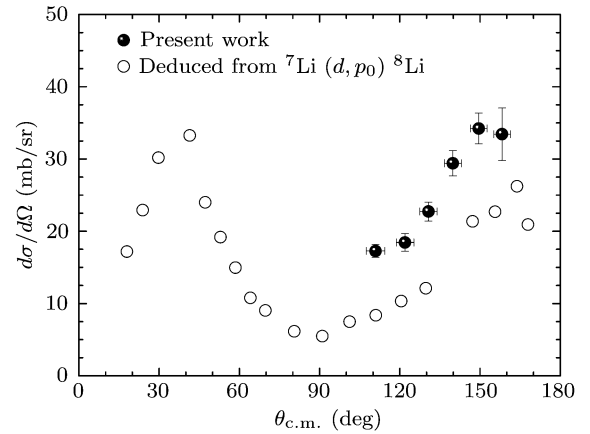


Fig. 3. ⁸Li(*p, d*)⁷Li angular distribution at $E_{c.m.} = 4.0$ MeV (full circles) and the ⁸Li(*p, d*)⁷Li angular distribution deduced from the ⁷Li(*d, p*)⁸Li reaction at $E_d = 5.03$ MeV (open circles).^[18]

The deuteron events from the ⁸Li(*p, d*)⁷Li reaction can be divided into two groups by their angles in the centre of mass frame. The deuterons at forward angles can not pass through DSSSD because of their low energies. The ⁸Li(*p, d*)⁷Li angular distribution only at backward angles is obtained, as shown in Fig. 3. The errors of differential cross section are mainly from the

statistics ($< 5\%$), and the uncertainties of beam normalization (4%) and areal density of hydrogen atoms in the $(\text{CH}_2)_n$ target (2%). The angular errors result from the beam spot size, the angular divergence of the secondary beam and angular spread generated when ^8Li passing through the ΔE detector and $(\text{CH}_2)_n$ target.

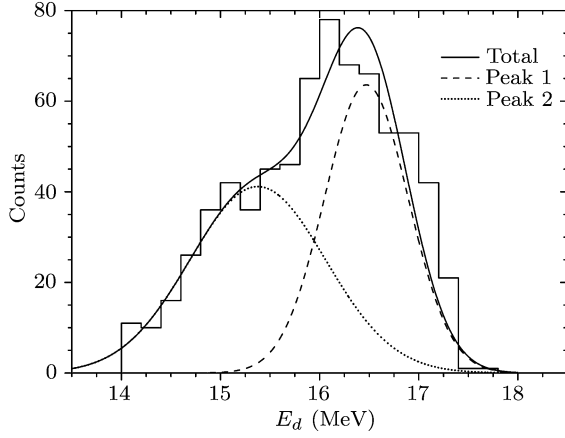


Fig. 4. Double Gaussian fit of the energy spectrum from some pixels of DSSSD with the equivalent radial position. Peaks 1 and 2 correspond to the ground state and first excited state in ^7Li , respectively.

Table 1. Parameters from the double Gaussian fit.

Curve	Parameter	Value	Error
Peak1	A_1	63.61	9.88
	x_1	16.47	0.074
	σ_1	0.423	0.035
	A_2	41.15	5.45
Peak2	x_2	15.38	0.16
	σ_2	0.685	0.084

The present result labelled with the full circles in Fig.3 includes the contributions from both $^8\text{Li}(p, d_0)^7\text{Li}$ and $^8\text{Li}(p, d_1)^7\text{Li}^*$. For estimating the ratio of these two components, the deuteron events from some pixels of DSSSD with the equivalent radial position are selected. A double Gaussian fit is made for the total energy spectrum of the selected events. The fitting results are shown in Fig. 4, in which Peaks 1 and 2 correspond to $^8\text{Li}(p, d_0)^7\text{Li}$ and $^8\text{Li}(p, d_1)^7\text{Li}^*$, respectively. The fitted parameters are listed in Table 1. The ratio mentioned above can then be extracted from these parameters. The $^8\text{Li}(p, d_0)^7\text{Li}$ contribution accounts for 40% ~ 58% in the mixture angular distribution. Both the fitting error and experimental uncertainties are taken into account in the calculation.

So far, there has been no published result on the $^8\text{Li}(p, d)^7\text{Li}$ reaction, the angular distribution of $^7\text{Li}(d, p_0)^8\text{Li}$ reaction at $E_d = 5.03\text{ MeV}$ by Mao *et*

al.^[18] is used for comparison. The corresponding centre of mass energy of its inverse process is 3.7 MeV, very close to that (4.0 MeV) in the present work. Based on the principle of detailed balance, the differential cross sections for a reaction $\sigma_{\alpha\beta}$ and its inverse reaction $\sigma_{\beta\alpha}$ are related by

$$\frac{\sigma_{\alpha\beta}}{\sigma_{\beta\alpha}} = \frac{\mu_\beta E'_\beta (2I_b + 1)(2I_B + 1)}{\mu_\alpha E'_\alpha (2I_a + 1)(2I_A + 1)}, \quad (2)$$

where μ_α , μ_β and E'_α , E'_β are reduced masses and the centre of mass energies for entrance channel and exit channel, respectively; I_a, I_A, I_b and I_B denote the spins of projectile, target, ejectile and residual nucleus respectively. The deduced angular distribution of the $^8\text{Li}(p, d_0)^7\text{Li}$ reaction is shown in Fig. 3, indicated by open circles. Its integral cross section at backward angles ($103^\circ < \theta_{\text{c.m.}} < 161^\circ$) is 51% ~ 62% of that obtained from our mixture angular distribution. This ratio is consistent with the fitting result on the $^8\text{Li}(p, d_0)^7\text{Li}$ component (40% ~ 58%) within the uncertainty.

In summary, the angular distribution of the $^8\text{Li}(p, d)^7\text{Li}$ reaction is measured in inverse kinematics at $E_{\text{c.m.}} = 4.0\text{ MeV}$ for the first time. The ratio of the contributions from $^8\text{Li}(p, d_0)^7\text{Li}$ and $^8\text{Li}(p, d_1)^7\text{Li}^*$ is then estimated through analysing the measured result. The $^8\text{Li}(p, d_0)^7\text{Li}$ component is approximately in agreement with the result deduced from the existing $^7\text{Li}(d, p_0)^8\text{Li}$ reaction data via the principle of detailed balance.

The authors thank the staff of the HI-13 tandem accelerator for their technical support during the experiment.

References

- [1] Alcock C et al 1987 *Astrophys. J.* **320** 439
- [2] Kajino T et al 1990 *Astrophys. J.* **359** 267
- [3] Cowan J J et al 1991 *Phys. Rep.* **208** 267
- [4] Qian Y Z 2003 *Prog. Part. Nucl. Phys.* **50** 153
- [5] Kajino T 1995 *Nucl. Phys. A* **588** 339
- [6] Wagoner R V et al 1967 *Astrophys. J.* **148** 3
- [7] Walker T P et al 1991 *Astrophys. J.* **376** 51
- [8] Miyatake H et al 2004 *Nucl. Phys. A* **738** 401
- [9] BalBes M J et al 1993 *Phys. Rev. Lett.* **71** 3931
- [10] BalBes M J et al 1995 *Nucl. Phys. A* **584** 315
- [11] Becchetti F D et al 1992 *Nucl. Phys. A* **550** 507
- [12] Li Z H et al 2005 *Phys. Rev. C* **71** 052801
- [13] Zeng S et al 2005 *Chin. Phys. Lett.* **22** 2219
- [14] Su J et al 2006 *Chin. Phys. Lett.* **23** 55
- [15] Bai X X et al 1995 *Nucl. Phys. A* **588** 273
- [16] Liu W P et al 2003 *Nucl. Instrum. Methods B* **204** 62
- [17] Tengblad O et al 2004 *Nucl. Instr. Methods A* **525** 458
- [18] Mao Zhenlin et al 1972 *Conf. on Low Energy Nucl. Phys. (Lanzhou)* p 3